Sorting of solid and soft objects in vortices driven by surface acoustic waves

Thomas Franke, Susanne Braunmüller, Thomas Frommelt, Achim Wixforth

Angaben zur Veröffentlichung / Publication details:

Franke, Thomas, Susanne Braunmüller, Thomas Frommelt, and Achim Wixforth. 2009. "Sorting of solid and soft objects in vortices driven by surface acoustic waves." In *Bioengineered and Bioinspired Systems IV: SPIE Europe Microtechnologies for the New Millennium, 4-6 May 2009, Dresden, Germany*, edited by Ángel B. Rodríguez-Vázquez, Ricardo A. Carmona-Galán, and Gustavo Liñán-Cembrano, 73650O. Bellingham, WA: SPIE. https://doi.org/10.1117/12.821701.

Sorting of solid and soft Objects in Vortices driven by Surface Acoustic Waves

Thomas Franke, Susanne Braunmüller, Thomas Frommelt, Achim Wixforth
Experimental Physics I, University of Augsburg, Universitätsstr. 1, 86159 Augsburg, Germany

ABSTRACT

A challenging topic of the lab-on-a-chip research is to implement sorting mechanisms on low cost disposable chips. In many applications, surface acoustic waves (SAW) have recently proven to be a versatile and efficient technique for microfluidic actuation. A SAW is excited by applying a high frequency signal to a piezoelectric substrate. When the wave hits the solid/liquid interface it transmits its acoustic energy into the liquid and a local pressure gradient emerges, leading to surface acoustic streaming. Experiments can be performed directly on the piezoelectric substrate or on a separate glass slide positioned on top of the SAW source. We developed a technique for the accumulation of solid and soft objects in SAW generated microvortices in microfluidic channels. For this purpose, the corner of a rectangular microchannel is irradiated by a wide SAW beam. There, the SAW excites sound waves in the fluid producing a typical acoustic streaming flow pattern which typically exhibits two vortices. Particles injected into the flow are accumulated and dynamically trapped in one of these vortices. After the flow is stopped, the collected particles stay in the position of the vortex. In our experiments, we use open microfluidic channels with functionalized hydrophilic-hydrophobic surfaces on glass substrates as well as closed channels build with the elastomer PDMS via soft lithography. We find that the accumulation efficiency for particles is strongly size dependent. Below a critical radius of 500 nm, particles tend to flow through the vortex and are not captured in the corner. Generally, larger particles can be collected at more moderate SAW power levels compared to smaller particles. Therefore, by adjusting the SAW power level, one is able to collect particles above a designated size. This concept is not limited to solid particles but can also be applied to soft objects like cells.

Keywords: Surface acoustic wave, microfluidics, particle accumulation, microvortices, biochip

1. INTRODUCTION

Miniaturized platforms and lab-on-a-chip devices for rapid point-of-care diagnostics are becoming increasingly important in clinical laboratories replacing conventional clinical laboratory analysis. A primary and essential step of most hematological clinical diagnostic is the extraction of blood cells and other cellular components from blood plasma. Conventional blood cell separation techniques such as centrifugation are generally time consuming and require comparatively large amounts of sample. For easy and accurate handling with conventional clinical laboratory pipettes reagents are required in sufficient amounts, usually several microliters. Additionally, effective centrifugation tools are difficult to implement on microscale dimensions. The application of porous filters as an alternative separation method deals with complex membranes or complicated fabrication techniques to achieve very small poresizes. Other drawbacks of filtering are pore plugging as well as large shear forces due to high pressures necessary to pump the fluid, which result in disadvantageous fragmentation of cells. Also, removing particles trapped in the filter, if they are the material of interest, is not always an easy task. Fast and efficient particle separation is not only required for blood component separation but also for biochemical and medical research and analysis. So called bead essays become more and more popular using antigen functionalized beads. Bead assays are used for example to purify proteins or, in analogy of an ELISA (Enzyme linked immunosorbent assay) plate, to detect other target molecules [1]. Whereas the signal detection in such ELISA bead assays is fully automated via fluorescently activated flow cytometers, sample preparation including several steps of bead centrifugation and resuspensation is still rather time- and manpower consuming. Implementing mechanisms on microfluidic devices to automatically collect and resuspend particles or cells would be of high value. Among current microfluidic approaches for particle separation is dielectrophoresis (DEP), which relies on the

Bioengineered and Bioinspired Systems IV, edited by Ángel B. Rodríguez-Vázquez, Ricardo A. Carmona-Galán, Gustavo Liñán-Cembrano, Proc. of SPIE, Vol. 7365, 73650O
 · doi: 10.1117/12.821701

polarizability of particles. As DEP particle velocities scale quadratically with the particle size this method is limited below 10 μm/s [2]. Other techniques use hydrodynamic focusing to continuously filter and separate blood components using rather complex channel geometries or comparatively large sample volumes[3,4]. Nevertheless, most of the microfluidic systems are confined and moved in tubes or capillaries. Usually, the application of such systems is restricted to continuous flow processes. As tubes need to be filled in order for the pump mechanism to work properly, very small amounts of liquids can not be handled. For some applications batch operation is preferred to continuous flow operation especially when the amount of sample has to be minimized [5]. A typical example would be the dissolving of a substance in a liquid or the exchange of the fluid of a suspended sample (e.g. washing step during purification).

In many miniaturized applications, surface acoustic waves (SAW) have recently proven to be a powerful and efficient technique for microfluidic actuation [6]. Recently we showed an efficient method for SAW driven acoustic mixing at low Reynolds numbers to overcome the diffusion limited mixing process in microfluidic systems [7]. Furthermore, surface acoustic waves can be used to actuate small liquid droplets or drive a flow in microchannels [8,9]. Here, we propose a SAW based effective mechanism to concentrate, trap or sort particles, blood components and other complex fluids. We show that the accumulation efficiency of particles in SAW induced vortices strongly dependent on their size.

2. METHODS

2.1 Surface acoustic waves

Surface acoustic waves were first described in combination with earthquakes [10]. Meanwhile surface acoustic waves are about to find their way into the field of microfluidic actuation for MEMs or lab-on-a-chip applications SAW devices have been used for years in communication circuitry. Actually, SAW devices are a huge industry in mobile communication widely used for RF signal processing and filter applications - every cell phones has filters using the effect.

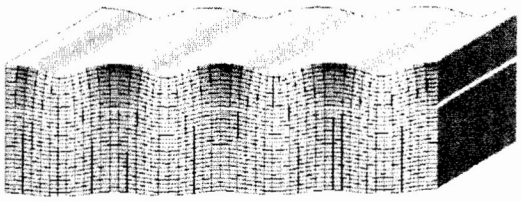

Fig. 1 Sketch of a SAW propagating on a piezoelectric substrate. Typical wavelengths are in the micrometer range, typical amplitudes are less than a nanometer. Alternating regions of compressed and expanded material are indicated in gray scale.

A SAWs of a well defined wavelength and frequency can be excited easily on piezoelectric substrates such as quartz, or Lithium Niobate ($LiNbO_3$), if a specially formed pair of comb-like structured electrodes is deposited on top of the substrate. Such electrodes are usually referred to as interdigital transducers (IDT). A high frequency electrical signal applied to such an IDT is then converted in a periodic deformation of the crystal underneath if the right frequency given by

$$f = v_{SAW}/\lambda \tag{1}$$

is employed. Here v_{SAW} denotes the sound velocity of the respective substrate, and the wavelength λ is given by the periodicity of the IDT structure. The SAW is confined to a thin layer at the surface of the substrate. Therefore SAW propagation crucially depends on boundary conditions at the surface. The sketch of a SAW propagating on a solid is

shown in Fig. 1 illustrating the characteristically alternating regions of compressed and expanded material. Typical wavelengths of SAW for microfluidic applications are around $\lambda = 30$ µm at $f \approx 100$ MHz.

As both mechanical as well as electrical load of the substrate surface significantly influences the SAW propagation, SAW devices can be employed as sensor elements or to measure the dynamic conductivity of thin film devices. Not only electrical interactions, but also mechanical interactions are a possible scope for experimental investigations, as most of the energy propagating in a SAW is mechanical in nature. Metaphorically speaking, a SAW can be described as a nano-earthquake with wavelength of a few microns and amplitudes of only a nanometer. The forces and electric fields within this nanoquake are sufficient to have a macroscopic effect. This macroscopic effect appears as vibrating force acting on any piece of matter on the surface in the path of a SAW. Liquids and other viscous materials absorb much of the SAW energy and it turns out that interaction between a SAW and a liquid on top of the substrate surface induces internal streaming.

2.2 Acoustic streaming

The basic mechanism of an acoustically induced internal streaming is illustrated in Fig. 2 with a SAW propagating from left to right along the x-axis. At x=0 the wave reaches the edge of a liquid at the surface of the substrate. With its non-vanishing amplitude in the z-direction, i. e. normal to the surface of the substrate, the SAW is then strongly absorbed by the fluid (leaky SAW). This is indicated by the decaying amplitude for positive x values in Fig. 2.

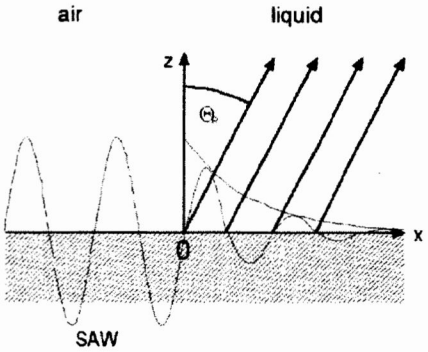

Fig. 2: Schematic illustration of the interaction between a SAW and a liquid on the surface of the substrate. The acoustic energy is radiated into the fluid from the left to the right and hits the liquid at x=0. Due to the different sound velocities in the substrate and in the liquid phase, the SAW leaks into the fluid under a refraction angle Θ_R leading to an internal streaming

The diffraction angle Θ_R at which the SA enters the liquid is determined by the difference in sound velocities for the solid substrate and the liquid, given by the following equation:

$$\Theta_R = \arcsin (v_S/v_f) \quad (2)$$

where v_s and v_f denote the sound velocities of the solid substrate and the fluid, respectively. This angle is also referred to as the Rayleigh angle. Additionally, an acoustic radiation pressure is generated acting in the direction of the sound propagation in the fluid. In closed liquid volumes like droplets, the actuated fluid is reflected back to its source at the boundaries causing internal streaming. The concept of internal streaming can be applied to effectively mix small volumes, or to circular liquid filled channels to drive the fluid [6].

2.3 Chip fabrication

Microfluidics with SAWs can be realized on open channels designs, where liquids are confined to virtual tracks simply by chemical modification of parts of the chip surface. For the preparation of such microfluidic chips, a $Y + 128°$ X-propagating $LiNbO_3$ piezoelectric Wafer (500 µm thick) was used as the substrate due to its high coupling coefficient in SAW generation. For the IDT structures and contact pads a thin layer of gold (typically 80 nm) is deposited on top of the substrate using standard lithography. To protect the IDTs from mechanical damage, a thin layer of SiO_2 (300 nm) was deposited on top of the IDTs. With common silanization techniques, we are able to create 2D hydrophilic patterns of preferred wettability separated by hydrophobic regions, where aqueous liquids are repelled. Thus, liquids are confined to desired geometries by surface tension. Most common lithographic techniques borrowed from semiconductor electronics comprises the silanization of specific areas of the surface where other regions of the surface are protected by laterally structured photoresists. In brief, the hydrophilic-hydrophobic structuring of the chip is done as following: an octadecyltrichlorsilane (OTS) layer was adsorbed to the surface by incubating the chip in silane-n-hexane mixture (24 µl of silane per 30 mL of hexane; Sigma-Aldrich, Taufkirchen, Germany) for 30 min. The silanization leads to complete hydrophobicity of the surface. After applying a thin layer of photoresist on top of the silane layer the surface was irradiated with UV light using a mask with the desired structure. Subsequent development removed the photoresist only at the exposed areas. After etching the chips in oxygen plasma and rinsing left-over photoresist with acetone, the hydrophilic-hydrophobic patterning is completed and the chips are ready to use. This simple but efficient method enables us to create easily a variety of virtual tracks oe reaction vessels on SAW chips to actuate and process liquid samples. In our experiments we used hydrophilic tracks similar to the shape of a racetrack. An IDT is placed in the vicinity of a corner of the track, as depicted in Fig. 3. The open channel microfluidic chip was mounted to a custom-made chip holder to connect the IDTs reversibly with the RF-source. To minimize liquid evaporation due to heating of the system during the experiments, a peltier element was implemented for active cooling. The chip holder is placed underneath a microscope to analyze the streaming effects.

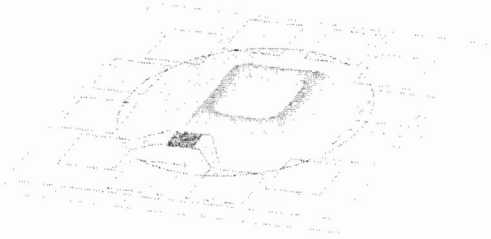

Fig. 3: 2D Open channel chip design with an IDT placed in the left corner of the fluidic track. The yellow squares are prefabricated gold contact pads, in this picture only two of them are used for IDT contacting. The fluid is constricted to the hydrophilic region, as indicated with the rectangular track in the middle of the chip, whereas the rest of the chip is rendered hydrophobic (pink circular area) via silanization.

Being a very versatile phenomenon, SAWs can also be applied to closed liquid volumes like square capillaries or channels. To create acoustic streaming in 3D microfluidic devices, which may consist of glass plastic or silicone, we simply place the device on top of the SAW generating piezoelectric substrate (Fig. 4). A drop of water filling the gap between SAW chip and the microfluidic device is added to efficiently couple the SAW into the glass devices. Closed channels used in our experiments were fabricated with the silicone elastomer PDMS [poly(dimethyl siloxan)]. A 10:1 mixture of elastomer:curing agent (Sylgard 184 Silicone Elastomer, Dow Corning, Germany) was mixed, degassed by placing in a vacuum for 30 min and poured on a SU-8 photoresist mold. After curing the PDMS for 3 h at 70°C the PDMS was peeled off and tightly sealed to a cover glass by oxygen plasma treatment. The SU-8 photoresist mold was fabricated performing lithography in the same manner as described above. The channel geometries used in our experiments had several 100 µm in width and up to 100 µm in height.

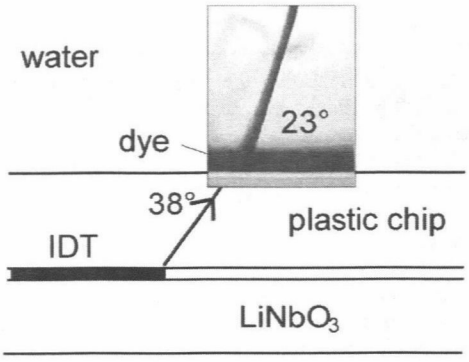

Fig. 4: SAW coupling through the bottom of a microfluidic chip (in this case polystyrene) into the fluid into the microfluidic channel on top. Depending on the different sound velocities in the different media the diffraction angle changes. In water the diffraction angle becomes visible by adding a small amount of dye, leading to a sharp jet after switching on the SAW (inset photograph).

3. EXPERIMENTAL RESULTS

In the following section we demonstrate the accumulation of solid particles in an open microfluidic channel geometry as shown in Fig. 3. The rectangular hydrophilic fluid track on the $LiNbO_3$ chip has 4 mm x 6mm. The hydrophilic area is filled with a small volume of distilled water (ca. 0.5µl) and completely covers the hydrophilic region of the chip. In order to visualize the fluid flow we added a small amount of latex beads (Molecular Probes Microspheres, Portland Oregon). To prevent evaporation the whole chip was cooled down to approx. 10°C. In close proximity to one corner of the rectangular fluid track an IDT was implemented to drive the micro-flow in a closed loop along the hydrophilic rectangular trajectory.

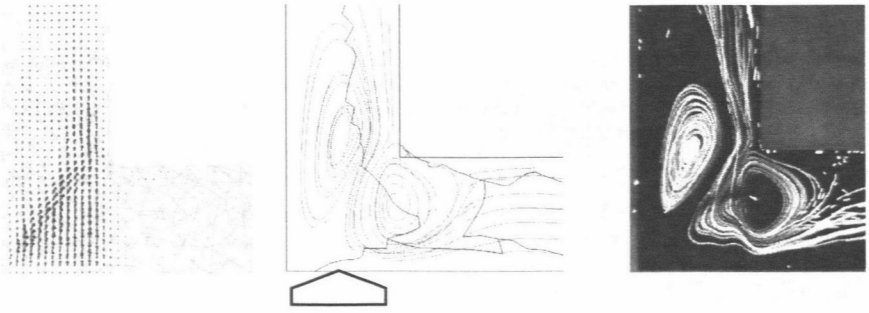

Fig. 5: The picture in the left shows experimental particle trajectories, in the middle theoretically obtained streamlines are depicted, the position of the IDT is indicated by the broad arrow [11]. Right picture: calculated force field arising from a wide SAW path.

We theoretically determined the fluid flow of the same geometry as in the experiment in a modified finite element method simulation [11]. To calculate the full 3 dimensional time dependent FEM solution of sound propagation is far behind what is computable. Therefore we separated the calculation into two sub-problems. First, we assume the coupling

of the propagating Rayleigh SAW into the fluid volume. The displacement normal to the piezoelectric surface leads to the most effective excitation of longitudinal acoustic waves into the fluid. Its angle is given by the Rayleigh angle as shown in Fig.2 . The irradiation of sound waves into the fluid and therefore loss in energy of the surface acoustic wave leads to attenuation and consequently a decay of its amplitude depending on the distance the wave has propagated below the liquid (leaky SAW). We estimate the characteristic length scale of attenuation of the SAW intensity to be l_{SAW} ~130μm [12]. Now, instead of solving the nonlinear set of hydrodynamic equations we consider a ray-tracing approach of sound wave propagation in the fluid. This can be justified from the fact that the acoustic wavelength is much shorter than the typical extension of the considered fluid volume [11]. At the boundaries between water and either the glas covered substrate or air the ray undergoes total reflection. Therefore, from the geometry of the liquid channel and the decay length L_{H2O}~2mm [13] the acoustic fluid velocity u can be calculated. According to the theory of acoustic streaming as discussed by Nyborg and Eckart [14,15] the acoustic fluid velocity causes a body force f acting on each fluid element. Details of this calculations are given in [14]. However, using this force field yields the velocity field from the stationary Stokes equation

$$-\nabla p + \eta \Delta v + f = 0 \tag{3}$$

and the incompressibility of the fluid.

A comparison of an experiment and theoretical simulation data for the same geometry is shown in fig. 4. An IDT with a wide SAW path (fwhm 490 +/- 10 μm) is placed near to the corner of a fluid channel. The resulting force field f is calculated from the SAW path and the coupling into the fluid. Due to multiple internal reflections at the free air-fluid and fluid-substrate boundaries a rather complex force field arises. The streaming pattern is obtained from the stationary Stokes equation applying this force field and displays two vortices as shown in fig. 4b. It exhibits excellent agreement as compared to the experiment in fig. 4c. Here, small tracer particles were used to visualize the fluid flow. However, there are some deviations from the theoretical flow trajectories in the region of strongest SAW intensities.

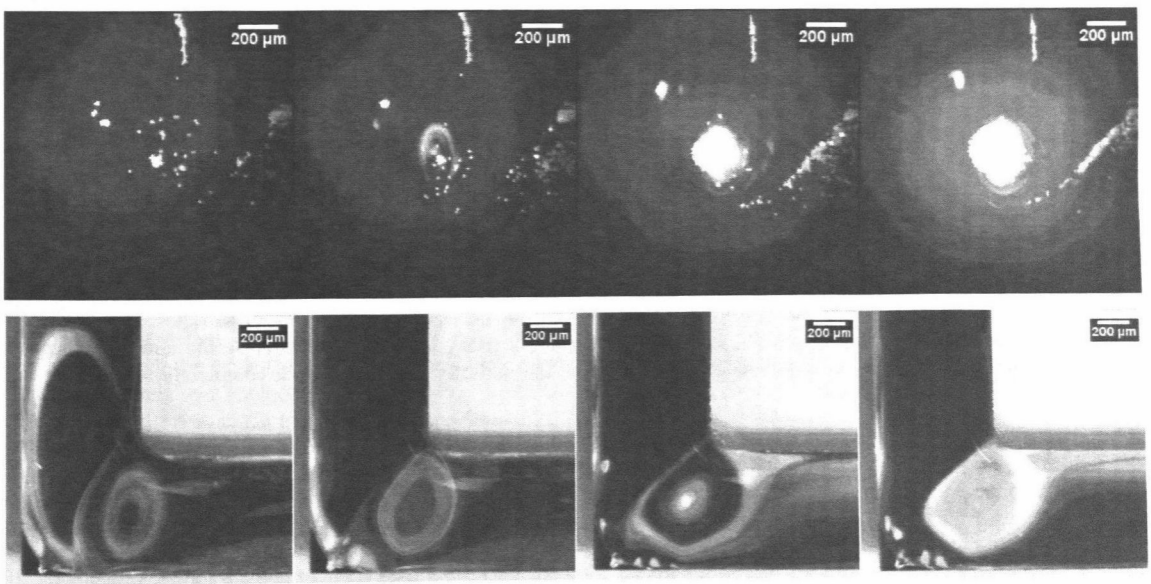

Fig. 6: upper panel: Micrographs of beads accumulating in a SAW induced vortex at moderate SAW power. Large beads (radius: r_p=4.8μm) successively accumulate with time. The sequence of snapshots is approx. 4s. The geometry of the fluidic chip is the shown in fig. 3. Particles are typically trapped in the lower vortex. lower row: Increasing the power of the surface acoustic wave intensity finally evokes accumulation of small beads of radius r_p=0.55μm (right micrograph).

To further investigate these differences we experimentally varied the SAW intensity and the diameter of tracer particles for the same geometry of microfluidics channel as before. Surprisingly, using Latex-tracer beads of a radius r_p=4.8μm we found that the beads accumulated with time in the right vortex as shown in Fig. 6 (upper panel). Smaller particles, as for example the ones used in Fig. 7 (right picture), do not accumulate at all at moderate SAW power. However, increasing the intensity of the surface acoustic wave, we were able to collect also beads of radii r_p=0.55μm. At smaller radii we could not successfully accumulate beads. The efficiency of accumulation obviously increases with intensity and diameter of the particles.

The size dependence of the accumulation effect is summarized in Fig. 7. After the streaming is switched off, the flow of the liquid stops immediately and the particles stay at their position. As can be seen in Fig. 7 the efficiency of the accumulation decreases dramatically below a critical particle radius of the order of r_p~0.5μm. This value corresponds to an estimation of Schindler[16]. By comparing the viscous drag and the compensating pressure gradient as take from theoretical estimation he was able to calculate a critical radius for accumulation of the same order (r_{crit}~0.5μm).

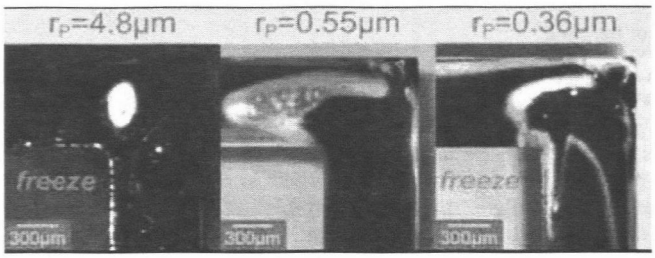

Fig. 7: Particle Size depend accumulation efficiency: larger particles (r =4.8 μm, left picture) are collected with high efficiency, whereas particles with a radius below 0.5 μm (right picture) are able to pass the vortex to some extend, even at high SAW power levels.

To complement and extend our experimental study, we applied the above concept of particle accumulation to conventionally used closed PDMS micro-channels. In comparison to open channel geometry the SAW now has to couple through a glass slide forming the bottom of the PDMS-glass composite. Furthermore, the boundary condition in the PDMS channels can be assumed to have non-slip boundary condition in contrast to the slip condition at the air-fluid boundary.

In the closed channel system, particle wall interactions play a more important role, because with increasing SAW power, particles collision with the channel walls are more likely to happen and may cause adhesion of particles. To minimized adhesion and immobilize the channel walls bovine serum albumin (BSA 1mg/ml) was added to the aqueous solution. After the SAW was switched off with continuing fluid flow, the particles could be almost completely washed off the walls indicating very low adhesion.

In order to separate larger from smaller sized particles, a mixture of particles with diameter of 5 μm and 0.5 μm were injected to a closed PDMS channel using syringes–driven pumps. Applying the SAW at one corner of the rectangular channel, the large-size particle fraction accumulates in the vortex, whereas the smaller ones still pass the vortex. This size dependent particle sorting is depicted in Fig. 8, where only the large particles are visible in bright-field microscopy (left picture). The smaller particles are fluorescently labeled and can therefore be visualized employing fluorescent microscopy (right picture). Obviously the small particles move through the vortex without being trapped permanently. If just one drop of the particle mixture is filled into the channel the flushed with water, the large particles can be separated from the small ones. After all of the small particles passed the vortex, switching off the SAW releases finally the large particles and they can be collected separately.

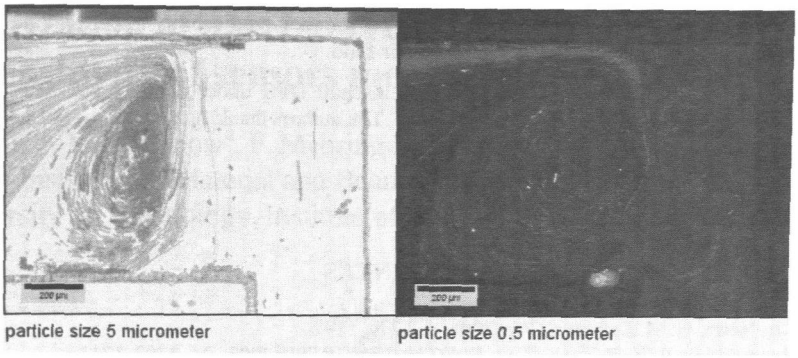

Fig. 8: The brightfield and fluorescent images of one experiment display sized dependent accumulation of particles in a closed channel: The fluid contains a mixture of particles with 5 μm diameter and 0.5 μm diameter. The larger particles are visible in brightfield microscopy only as shown in the left picture. The smaller particles are below the resolution limit and are therefore not visible in the left picture. However, the small particles are coated with a fluorescent dye and visible in fluorescent microscopy (right picture). Only the larger particles are concentrated in the region of the vortex (left picture) while the smaller particles disperse almost homogeneously (right picture).

4. DISCUSSION AND CONCLUSION

Here, we showed a simple yet effective and versatile method to concentrate, filter or sort suspended particles in microfluidic channels. We found the efficiency of particle accumulation to depend on several independent parameters. First, the channel geometry has an impact on the accumulation effect. More efficient particle collection was found in rectangular channels with sharp corners compared to round off corner geometries. Second, the diameter of the particles is also a major criterion. With increasing particle size the accumulation was more effective. However, last not least also small particles above a critical size of approx. r_p~0.5μm could be successfully accumulated when the power of the SAW intensity was increased. To conclude larger particles are collected at comparatively lower SAW power levels, smaller particles require larger SAW power levels to achieve the same accumulation efficiency. However, our experimental results suggest a critical value for particle size. Particles with a diameter below 0.5 μm could not be trapped efficiently in the region of the vortex. In a theoretical study combining a ray tracing algorithm and FEM simulations, we were able to gain quantitative agreement with the experimental data of fluid flow. Furthermore, the critical radius for particle aggregation found experimentally, could be explained recently by another group [16].

We demonstrated that both, an open and closed channel designs are suitable to concentrate or sort different sized particles. Among the advantages of open microfluidic channel designs, as presented here, are their easy accessibility and the comparatively low contact of the sample fluid to device surfaces. As in clinical research and laboratory application, often a huge effort is made to minimize unspecific interactions of desired proteins or other molecules of interest with glass or plastic surfaces. However, open channels with a large air-liquid interface exhibit increased evaporation rates of water, which might be unfavorable for some applications. A simple method to minimize evaporation in open channels is to cover the fluid with mineral oil. The problem of water evaporation is circumvented by using closed channels. Interactions between channel walls and particle can be minimized by treatment with simple coating agents like polyethylene glycol (PEG) or bovine serum albumine (BSA). Furthermore, compared to the open channel chip design, larger volumes can be processed. This system is therefore advantageous for concentration of highly diluted solutions or for efficient purification of particles.

Further possible applications of SAW based sorting devices are the separation blood cells from plasma or even the isolation of migrating tumor cells from the blood stream during tumor metastasis. Furthermore, immunoassay bead based techniques which are commonly used in clinical research and diagnosis, promise to be an interesting area of application. Such bead assays include several steps of centrifugation and pipetting to wash the samples and to exchange the reaction solutions. Those time-consuming protocols restrict the reliability and the sensitivity of the bead assays. SAW based

devices may offer a powerful solution to this problem, as we proved their applicability to concentrate particle solutions and hold the particles in a position during exchange of the outer fluid.

This work was supported by the Deutsche Forschungsgemeinschaft DFG under contract No. SPP 1164 and by the German government through the Cluster of Excellence "NIM".The authors thank A. Spoerhase, S. Lieber and A. Hupfer for their technical assistance.

REFERENCES

(1) Wiklund, M.; Hertz, H. M. *Lab on a Chip* **2006**, *6*, 1279-1292.
(2) Adrienne R. Minerick, R. Z. P. T. H.-C. C. *ELECTROPHORESIS* **2003**, *24*, 3703-3717.
(3) Choi, S.; Song, S.; Choi, C.; Park, J. *Lab Chip* **2007**, *7*, 1532-1538.
(4) Faivre, M.; Abkarian, M.; Bickraj, K.; Stone, H. A. *Biorheology* **2006**, *43*, 147-159.
(5) Geschke, O.; Klank, H.; Telleman, P. In *Microsystem Engineering of Lab-on-a-chip Devices*; Wiley-VCH: Weinheim, 2004.
(6) Wixforth, A. *JALA* **2006**, *11*, 399-405.
(7) Sritharan, K.; Strobl, C. J.; Schneider, M. F.; Wixforth, A.; Guttenberg, Z. *Applied Physics Letters* **2006**, *88*, 054102-3.
(8) Wixforth, A.; Strobl, C. J.; Gauer, C.; Toegl, A.; Scriba, J.; Guttenberg, Z. *Anal Bioanal Chem* **2004**, *379*, 982-991.
(9) Matthias F. Schneider, Z. G. S. W. S. K. S. V. M. M. U. P. A. W. *ChemPhysChem* **2008**, *9*, 641-645.
(10) Lord Rayleigh, J. W. S. *Proceedings of the London Mathematical Society* **1885**, *17*, 4.
(11) Frommelt, T.; Gogel, D.; Kostur, M.; Talkner, P.; Hanggi, P.; Wixforth, A. *Ultrasonics, Ferroelectrics and Frequency Control, IEEE Transactions on* **2008**, *55*, 2298-2305.
(12) Dransfeld, K.; Salzmann, E. In *Physical Acoustics*; Mason, W. P., Thurston, R. N., Eds.; Academic Press: New York, 1970.
(13) Coates, R. F. W. *Underwater acoustic waves*; Wiley: New York, 1989.
(14) Nyborg, W. L. In *Physical Acoustics, Properties of polymers and nonlinear acoustics*; Mason, W. P., Ed.; Academic Press: New York, 1965; Vol. 2B.
(15) Eckart, C. *Physical Review* **1948**, *73*, 68.
(16) Schindler, M., Universität Augsburg, Dissertation, 2006.